Electronic Supplementary Material (ESI) for Journal of Materials Chemistry A.

Supporting Information

Discarded cigarette filters-derived hierarchically porous carbon@graphene composites for lithium-sulfur batteries

Hongbin Xu,[a] Yang Liu,[b] Qianyun Bai,[a] Renbing Wu[a,c,d]*

Experimental Section

Preparation of Graphene Oxide (GO).

GO was prepared based on the modified Hummers' method.

Preparation of PC@G, PC and G.

Waste cigarette filters (CFs) were collected with wrapped papers removed in advance. The CFs were rinsed by deionized water and then were immersed in the GO suspension (7 mg mL^{-1}) for 6 h. After that, CFs@GO composites were placed in the refrigerator at −4 °C overnight and dried in a freeze dryer with a vacuum at −50 °C for 24 h. Finally, the composites were heated to 900 °C with the rate of 5 °C min^{-1} to get PC@G. For comparison, we also synthesized PC and G by similar methods but using bare CFs and GO, respectively.

Preparation of PC@G/S, PC/S, G/S.

The PC@G/S composite was prepared via a melt-diffusion method. Typically, a mixture of sublimed sulfur and PC@G with a mass ratio of 4:1 was sealed in a glass bottle, and heated at 155 °C for 12 h in an oven. PC/S and G/S were prepared in a similar way.

Materials characterization

The phase of the as-prepared composites was identified using a powder X-ray diffraction (XRD, D8 ADVANCE X-ray diffractometer) system with Cu Kα radiation. The field emission scanning electron microscope (FESEM, ZEIS, Ultra-55) and transmission electron microscope (TEM, JEOL JEM-2100F) were used to investigate morphologies and microstructures of the composites. Noted that the FESEM systems were equipped with energy-dispersive X-ray (EDX) spectroscopy. The chemical states of the elements in composites were revealed by X-ray photoelectron spectroscopy (XPS, XSAM-800 spectrometer with an Mg Kα radiation source). Raman spectra were recorded on an Invia/Reflrx Laser Micro-Raman spectroscope. The specific surface area and the pore-size distribution of the as-prepared composites was determined by nitrogen sorption isotherm at 77 K (ASAP 2020 Plus HD88 instrument). Thermogravimetric analysis (TGA) measurements were carried out on a Netzsch STA 449C

thermal analyzer from room temperature to 500 °C at a heating rate of 10 °C min^{-1} in a N_2 atmosphere.

Electrochemical measurements

The electrochemical performance was evaluated using CR2032 coin-type cells. The cathode was fabricated by mixing the as-prepared PC@G/S, carbon nanotubes (CNTs) and polyvinylidene fluoride (PVDF) in a weight ratio of 8:1:1 in N-methyl-2-pyrrolidinone solvent. The resulting slurry was then coated onto aluminium foil followed by drying under vacuum at 50 °C for 12 h. The loading density of sulfur was ~ 2.0 mg cm^{-2}. The anode was Li metal and the separator was Celgard-2300. The electrolyte was 1.0 M bis(trifluoromethane)sulfonimide lithium salt (LiTFSI) in a 1:1 (v/v) mixture of 1,2-dimethoxyehane (DME) and 1,3-dioxolane (DOL) containing 1.0 wt% $LiNO_3$. The amount ratio of electrolyte/sulfur was 20 μL:1 mg and therefore the volume of the electrolyte used in each cell was ranging from 30 to 50 μL. The galvanostatic charge and discharge tests were carried out on a LAND CT2001 testing system at the voltage window of 1.7−2.8 V. Cyclic voltammetry (CV) was determined on a CHI 760E electrochemical workstation (Shanghai, China) in the voltage range of 1.7−2.8 V at a scan rate of 0.1 mV s^{-1}. Electrochemical impedance spectroscopy (EIS) measurements were carried out on an electrochemical workstation (AutoLab PGSTAT302N) in the frequency range from 100 kHz to 0.01Hz. 0.2 M Li_2S_6 was dissolved in DME/DOL (v/v, 1:1) and diluted to 0.002 M for the adsorption test. All the absorbents (10 mg) were dried in vacuum oven before adding into the Li_2S_6 solution. The sealed vials were kept in glove box overnight, and then the liquid supernatants were used for the UV–visible absorption spectrophotometry (UV–vis, Varian Cary 100 Conc).

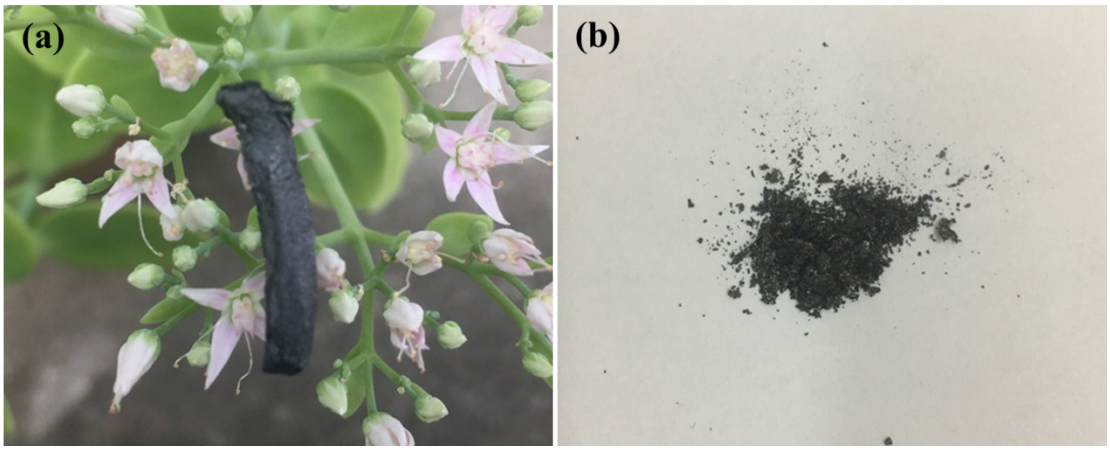

Fig. S1 Photograph of (a) cigarette filters-derived PC@G and (b) cigarette filters-derived PC composites.

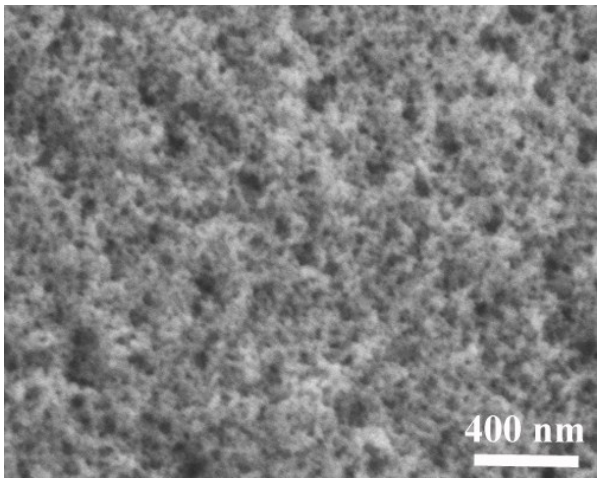

Fig. S2 Cross-section FESEM image of PC@G composite.

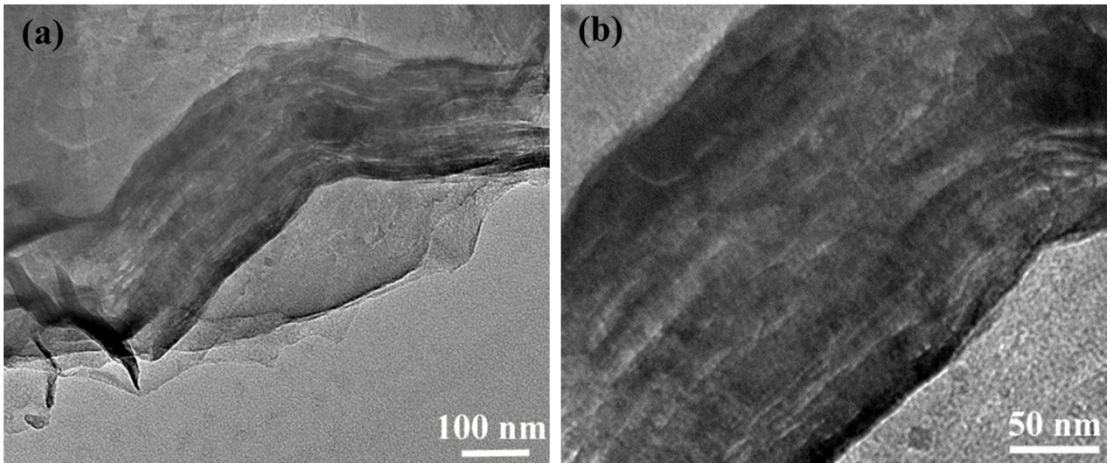

Fig. S3 (a) and (b) TEM images of PC@G composite.

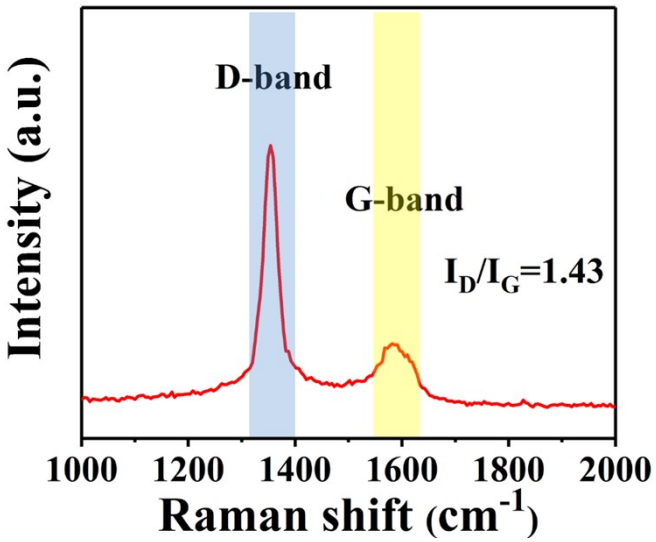

Fig. S4 Raman spectrum of cigarette filters-derived PC.

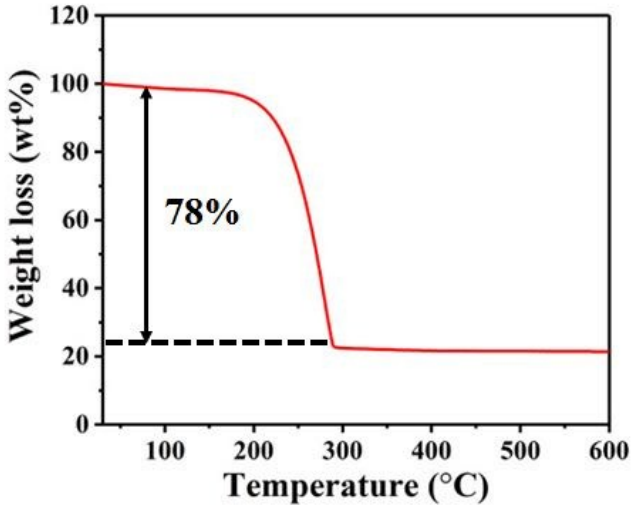

Fig. S5 TGA curve of PC@G/S composites.

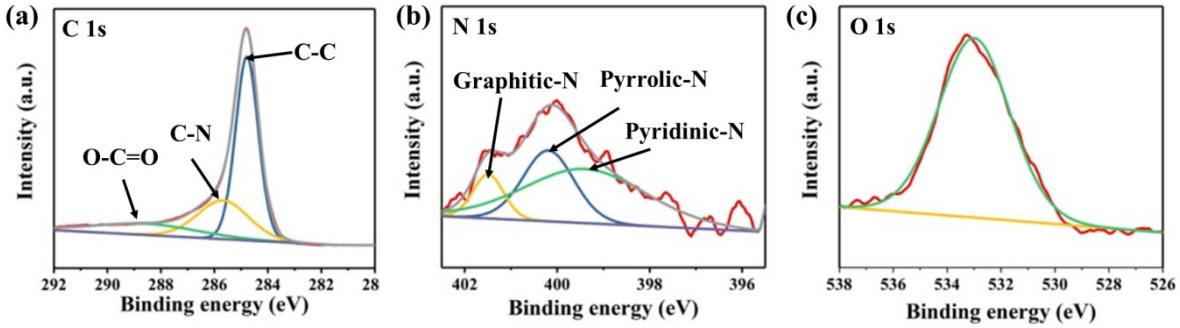

Fig. S6 XPS spectra of PC@G: (a) C 1s, (b) N 1s and (c) O 1s.

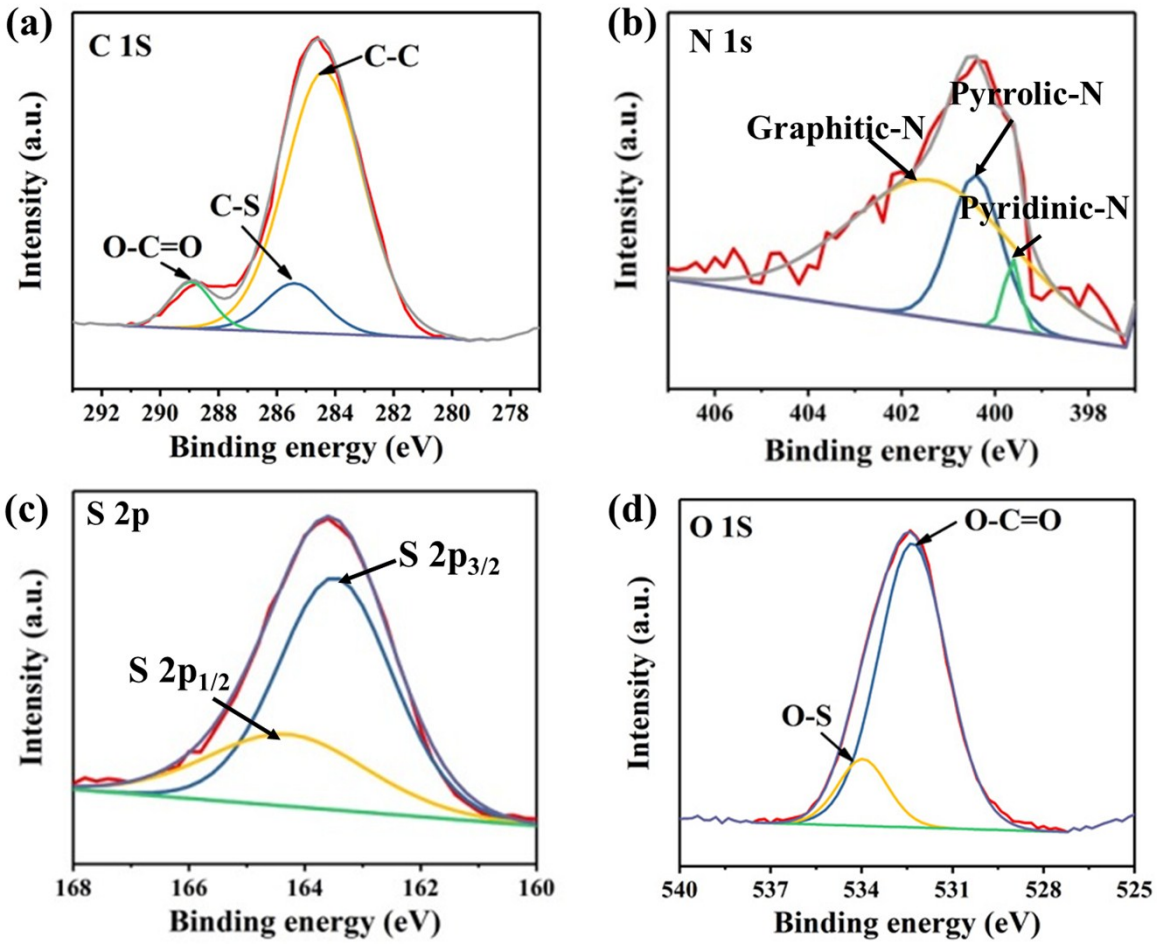

Fig. S7 XPS spectra of PC@G/S: (a) C 1s,(b) N 1s, (c) S 2p and (d) O 1s.

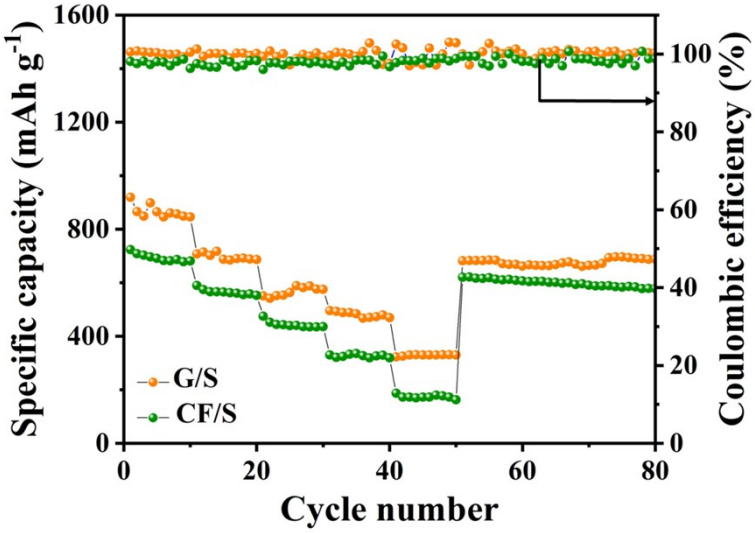

Fig. S8 Rate capabilities and corresponding coulombic efficiencies of G@S and PC@S cathodes at various current densities from 0.1 to 2.0 C.

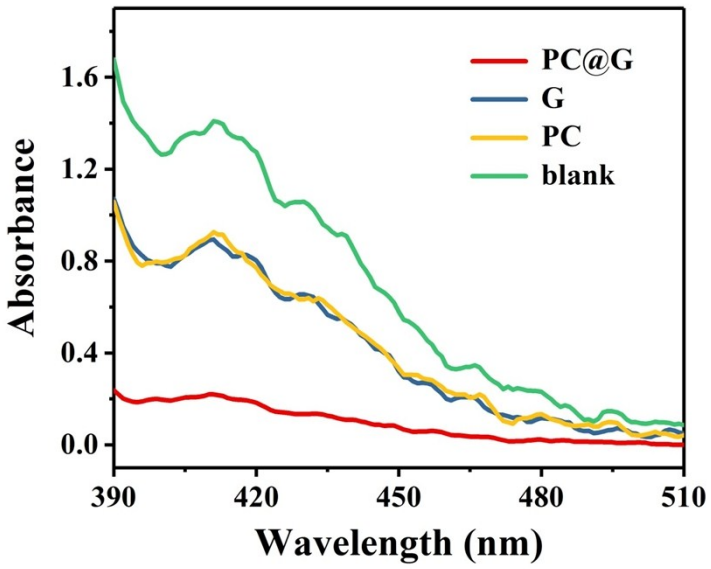

Fig. S9 UV–vis adsorption spectra of polysulfide solutions absorbed by PC@G, G, and PC.

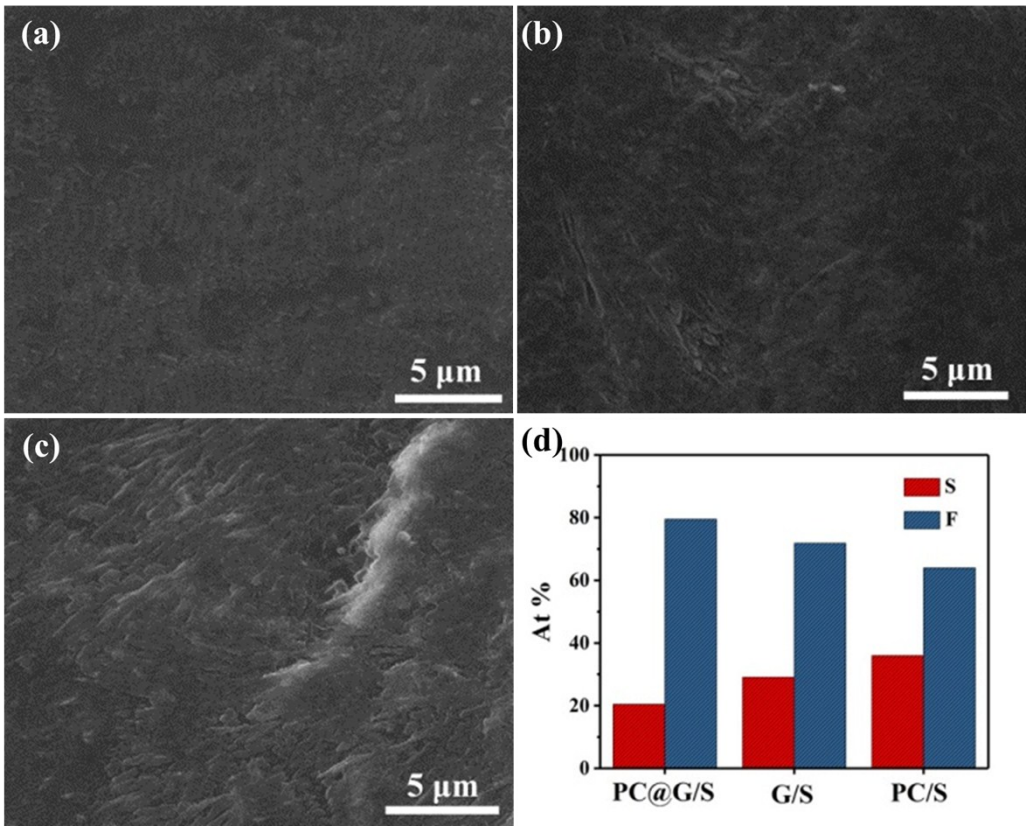

Fig. S10 FESEM images of Li anodes of Li-S batteries using (a) PC@G/S, (b) G/S and (c) PC/S cathodes after 100 cycles. (d) EDS results of elemental S and F recorded from different Li anodes after 100 cycles.

Table S1. Comparison of electrochemical performances of PC@G@S composites cathode with previously reported carbon-based cathodes.

Material	Electrode Formulation[a]	Cycling stability (A/B/n)[b]	Ref.
GN-CNT@S	7:2:1	463.7/0.5/500	[S1]
PRC@Ni@S	8:1:1	821/0.2/500	[S2]
PGPC@Ni@S	8:1:1	1030/0.2/200	[S3]
NCNT@G@S	8:1:1	896/0.5/200	[S4]
M-MGCSs@S	8:1:1	908/0.2/100	[S5]
NMCNFs@S	8:1:1	636/0.1/500	[S6]
rGO@PC@S	8:1:1	848/1.0/300	[S7]
POF-HS@S	8:1:1	773/0.5/200	[S8]
GC-PC@Co@S	8:1:1	790/0.2/220	[S8]
N-PCNSs@Co@S	8:1:1	913/0.2/100	[S9]
PCS@S	8:1:1	1013/0.2/50	[S10]
PCNF@CNT@S	8:1:1	798.5/0.5/200	[S11]
GLC@S	8:1:1	504/1.0/400	[S12]
N-SWCNH@S	8:1:1	573/0.1/200	[S13]
PC-CNT@S	8:1:1	932.8/0.5/150	[S14]
PC@G@S	8:1:1	1010.4/0.2/200	Our work
PC@G@S	8:1:1	721.9/0.5/1000	Our work
PC@G@S	8:1:1	508.4/1.0/1000	Our work

[a] Weight ratio of the active material, carbon and binder.

[b] A/B/*n* means the capacity of A (mAh g^{-1}) remained after *n* cycles at the certain current density of B (C).

References

1 Z. Zhang, L. L. Kong, S. Liu, G. R. Li, X. P. Gao, *Adv. Energy Mater.* 2017, **7**, 1602543.

2 Y. Zhong, X. H. Xia, S. J. Deng, J. Y. Zhan, R. Y. Fang, Y. Xia, X. L. Wang, Q. Zhang, J. P. Tu, *Adv. Energy Mater.* 2018, **8**, 1701110.

3 X. Q. Zhang, Y. Zhong, X. H. Xia, Y. Xia, D. H. Wang, C. A. Zhou, W. J. Tang, X. L. Wang, J. B. Wu, J. P. Tu, *ACS Appl. Mater. Interfaces* 2018, **10**, 13598−13605.

4 Y. Ding, P. Kopold, K. Hahn, P. A. van Aken, J. Maier, Y. Yu, *Adv. Funct. Mater.* 2016, **26**, 1112-1119.

5 J. H. Zheng, G. N. Guo, H. W. Li, L. Wang, B. W. Wang, H. J. Yu, Y. C. Yan, D. Yang, A. G. Dong, *ACS Energy Lett.* 2017**, 2**, 1105-1114.

6 Y. C. Yao, P. Liu, Q. Zhang, S. Z. Zeng, S. S. Chen, G. J. Zou, J. Z. Zou, X. R. Zeng, X. H. Li, *Mater. Lett.* 2018, **231**, 159-162.

7 H. Zhang, Q. M. Gao, W. W. Qian, H. Xiao, Z. Y. Li, L. Ma, X. H. Tian, *ACS Appl. Mater. Interfaces*, 2018, **10**, 18726–18733.

8 B.-Q. Li, S.-Y. Zhang, L. Kong, H.-J. Peng, Q. *Adv. Mater.* 2018, **30**, 1707483.

9 Y. Q. Lu, Y. J. Wu, T. Sheng, X. X. Peng, Z. G. Gao, S. J. Zhang, L. Deng, R. Nie, J. Swiatowska, J. T. Li, Y. Zhou, L. Huang, X. D. Zhou, S. G. Sun, *ACS Appl. Mater. Interfaces*, 2018, **10 (16)**, 13499–13508.

10 S. H. Liu, J. Li, X. Yan, Q. F. Su, Y. H. Lu, J. S. Qiu, Z. Y. Wang, X. D. Lin, J. L. Huang, R. L. Liu, B. N. Zheng, L. Y. Chen, R. W. Fu, D. C. Wu, *Adv. Mater.* 2018, **30**, 1706895.

11 G. Li, W. Lei, D. Luo, Y.-P. Deng, D. Wang, Z. Chen, *Adv. Energy Mater.* 2018, **8**, 1702381.

12 Y. Z. Zhang, Z. Zhang, S. Liu, G. R. Li, X. P. Gao, *ACS Appl. Mater. Interfaces*, 2018, **10**,

8749–8757.

13 H. W. Du, X. C. Gui, R. L. Yang, Z. Q. Lin, B. H. Liang, W. J. Chen, Y. J. Zheng, H. Zhu, J. Chen, *Nanoscale*, 2018, **10**, 3877-3883

14 U. Gulzar, T. Li, X. Bai, M. Colombo, A. Ansaldo, S. Marras, M. Prato, S. Goriparti, C. Capiglia, R. P. Zaccaria, *ACS Appl. Mater. Interfaces*, 2018, **10**, 5551–5559.

15 W. Yang, W. Yang, A. L. Song, G. Sun, G. J. Shao, *Nanoscale*, 2018, **10**, 816-824.